Investigating Alteration Zone Mapping Using EO-1 Hyperion Imagery and Airborne Geophysics Data

M. Lotfi[1*], H. Arefi[1*] and A. Bahroudi[2]

1-School of Surveying and Geospatial Engineering, College of Engineering, University of Tehran, Tehran, Iran
2-School of Mining Engineering, College of Engineering, University of Tehran, Tehran, Iran

Keywords	Abstract
Hyperspectral imagery *Geophysical data* *Alteration mapping* *SAM algorithm* *Hyperion data.*	Hyperspectral remote sensing records reflectance or emittance data in a large sum of contiguous and narrow spectral bands, and thus has many information in detecting and mapping the mineral zones. On the other hand, the geological and geophysical data gives us some other fruitful information about the physical characteristics of soil and minerals that have been recorded from the surface. The Sarcheshmeh mining area located in the NW-trending Uromieh-Dokhtar magmatic belt within Central Iran is mainly of porphyry type, and is associated with extensive hydrothermal alterations. Due to the semi-arid type of climate with abundant rock exposure, this area is suitable for application of remote sensing techniques. In this work, we focus on generating the alteration maps around Cu porphyry copper deposits using the spectral angle mapper algorithm on Hyperion data by applying two filters named reduction to pole and analytical signal on a total magnetic intensity map and generating the Kd map from radiometry data. What is clear is the high importance of applying the adequate pre-processing on Hyperion data because of low signal-to-noise ratio. By comparing the known deposits in the region with the results obtained by applying the mentioned methods, it is revealed that not all the higher K radiometric values are entirely associated with the hydrothermal alteration zones, and in contrast, the potassic alteration map extracted from Hyperion imagery successfully corresponds to the alteration zones around the Sarcheshmeh mining area. Finally, the results particularly obtained from processing the Hyperion data are confirmed by indices of Cu porphyry deposits in the region.

1. Introduction

A large number of magmatic intrusive bodies and mineral deposits emplaced in many regions of the earth made the researchers to study new methods to explore the mining areas by spending low money, time, energy, etc. Generally, mineral exploration is a multi-disciplinary task requiring the simultaneous consideration of numerous geophysical, geological, and geochemical datasets [1]. Hyperspectral remote sensing acquiring reflectance or emittance data in many contiguous and narrow spectral bands provides near-laboratory quality reflectance spectra, and indicates a new era of remote sensing. Airborne and space borne hyperspectral data has been used by the researchers for mineral mapping and discriminating the alteration zones [2-4]. Hosseinjani Zadeh *et al.* have implemented a partial sub-pixel method, the Mixture Tuned Matched Filter (MTMF), on a pre-processed and calibrated Hyperion dataset, and finally, verified the results by testing the area. The characteristic alteration minerals identified by Hyperion data included biotite, muscovite, illite, kaolinite, goethite, hematite, jarosite, pyrophyllite, and chlorite [5]. The results of a research work focused on the application of HyMap airborne hyperspectral data and ASTER satellite multispectral data for mineral exploration and lithologic mapping showed a detailed picture (produced by analysis on HyMap data) of the spatial distribution of the alteration minerals in an

unavailable area from field-based studies and mineral maps. The ASTER imagery can be useful for reconnaissance level mineral exploration due to its moderate spatial and spectral resolution [3].

The gamma ray spectrometry method is widely used in geological mapping [6, 7], mineral exploration [8-10], and soil mapping [11]. It involves the measurement of the naturally occurring radioactive elements uranium (U), thorium (Th), and potassium (K) for the outer most part of the Earth's surface, where the rock forming minerals and soil profiles exist [12].

Shives *et al*. have used airborne and ground gamma-ray spectrometry to detect and map potassium alteration associated with polymetallic volcanic-hosted massive sulfides (VMSs), magmatic–hydrothermal deposits (Au–Co–Cu–Bi–W–As), and porphyry Cu–Au–(Mo) deposits. The results of the research work showed that the potassium enrichment in these geological settings was characterized by anomalously low eTh/K ratios relative to normal lithological signatures, and thus it could be utilized as an important exploration indicator [13].

Airborne magnetic surveys, which are rapid and economic, have been traditionally employed for exploration of the porphyry-Cu deposits. Porphyry intrusions and the related alteration systems may have a characteristic magnetic signature, which can form a distinctive anomalous pattern in magnetic maps [14-16].

Therefore, in this research work, we decided to use the magnetic, radiometric, and Hyperion data so that the alteration maps could be generated.

Moreover, by means of known mines and deposit in the region, accuracy assessment was carried out.

2. Geology overview
In this work, we aimed to detect a porphyry copper mineralization area in the Uromiyeh-Dokhtar magmatic arc in the Central Iran zone, Kerman Province (Iran) within the coordinates of 55°52′–55°54′E and 29°48′–30°00′N. The whole studied area and distribution of different geological features are shown in Figure 1. In this region, there are some of the largest porphyry copper mines of Iran, i.e. Sarcheshmeh. Moreover, there exist the Darrehzar mine and Sereidun deposit. It is considerable that Sarcheshmeh is characterized by the alteration zones.

The concentric alteration zones at the Sarcheshmeh mine from the center to outward are potassic, biotitic, phyllic, argillic, and propylitic [17]. This pattern is the same as the typical alteration enveloping other porphyry Cu deposits [18].

The alteration types at the Sereidun deposit are manifested by the early chlorite-epidote (propylitic), transitional quartz-sericite (phyllic), quartz-clay (argillic), late quartz–alunite–pyrophyllite (advanced argillic), and quartz pyrophyllite (silicic) [5].

Mineralization in the Darrehzar copper mine is associated with diorite and granodiorite along with their enclosing Eocene volcano-sedimentary rocks. Both intrusions and their host rocks are extensively altered by hydrothermal fluids into potassic, phyllic, propylitic, and argillic assemblages [5].

Table 1. Summary of geophysical and remote sensing methods and their characteristics applicable to exploration and geoenvironmental studies [19]. [In method column: A, airborne surveys; B, borehole surveys; and G, ground surveys.]

| Method	Physical parameter measured	Typical units	Relevant physical property	Typical source of anomaly	Depth of investigation
Magnetic: A, B, G	Vector component or total attraction of Earth's magnetic field	Nanotesla, or gammas	Magnetic susceptibility and remanent magnetization	Magnetic susceptibility and (or) remanent magnetization contrasts	Surface to Curie isotherm
	Gradient of Earth's magnetic field	Nanotesla/m	"	"	
Gamma-ray spectro-metry: A, B, G	Rate of gamma-ray photons received and their energy	Counts/sec-ond in spectral regions. If calibrated, %K and PPM equiv. U and Th	Quantity of K, U, Th and daughters	K, U, and Th contrasts in Earth's upper 50 cm	Upper 50 cm
Remote sensing: A	Reflected radiation Intensity (UV, visible, IR)	Recorded as optical or digital intensity image	Spectral reflectance, Albedo	Changes in spectral reflectance and albedo	Surface only
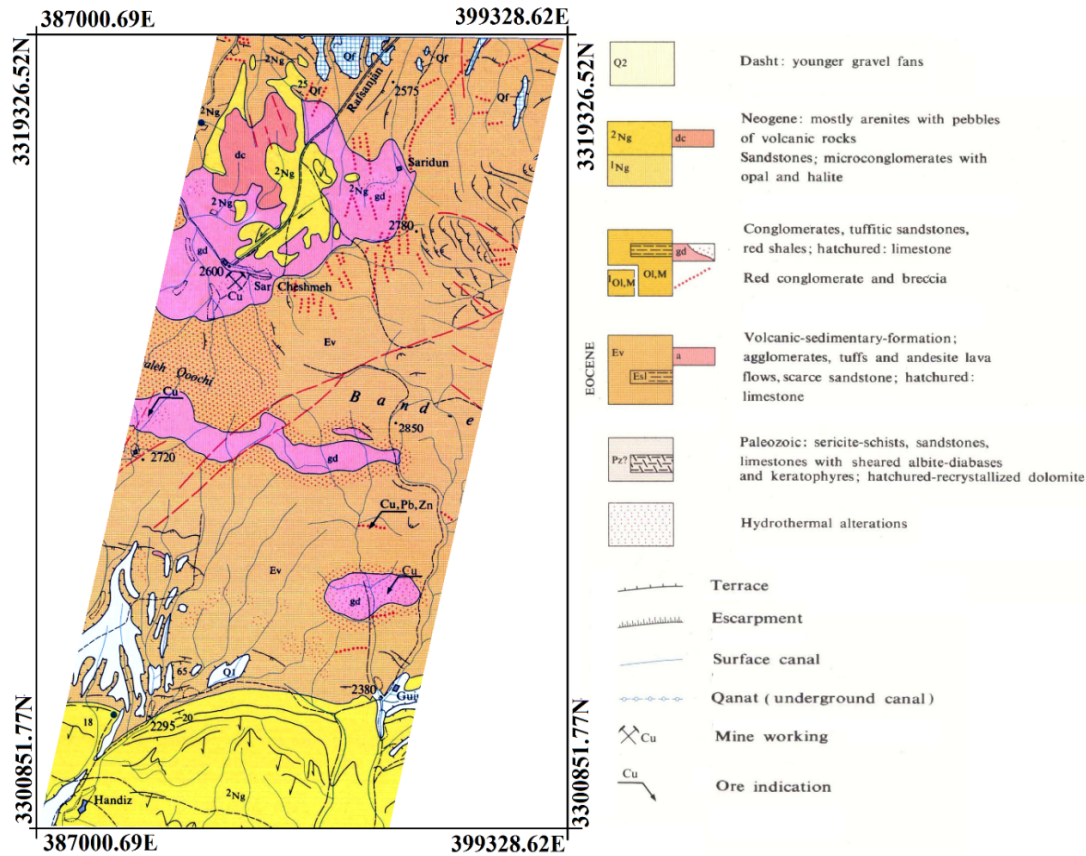
Figure 1. Geological map of the studied area (zone 40 in UTM system).

3. Materials and methods
In this work, a total magnetic intensity map as well as the radiometry data, provided by Atomic Energy Organization of Iran between years of 1974 and 1977, were utilized as the geophysical materials. It is important to mention that the flight height and the distance between the flight lines, with the azimuth angle of 225.45 degrees, were 120 m and 500 m, respectively. Moreover, Hyperion imagery was used as the remotely-sensed data. The specific features of the methods are given in Table 1.

3.1. Analysis on geophysics data
3.1.1. Introduction of geophysical methods
Magnetic data is commonly used for interpretation of granitoid bodies. Moreover, it is possible to distinguish the lateral extent of plutonic bodies from their associated magnetic signatures using processed magnetic data to identify boundary features. There are several filters including downward continuation, horizontal and vertical derivatives, tilt angle, and other forms of high-pass filters to enhance the magnetic field data. Among them, the analytic signal method is a highly popular one [15]. In this research work, according to making use of remotely-sensed data, Hyperion

imagery, and since they can just investigate the surface features of the earth, the analytical signal method due to minimizing deep anomalies and highlighting the surface ones were applied. The basic concepts of the analytic signal method for magnetic data were discussed extensively by Nabighian [20, 21].

In the studied region, unlike the strong relation between the K concentration and hydrothermal zones, there was no relationship between U and Th accumulations with hydrothermal processes. Therefore, it may be possible to determine the hydrothermalized areas through suppressing the areas associated with the U and Th values in contrast to the regions related to K enrichment. In order to achieve this aim, the Kd map was obtained based on the following relations [22].

$$Ki = (K \text{ map average/Th map average}) \times Th \text{ map} \quad (1)$$

Since Ki shows the ideal potassium value, anomalies of real values from ideal values were obtained by the equation bellow:

$$Kd = (K − Ki)/Ki \quad (2)$$

The obtained value represents K distribution, which may be related to the hydrothermal areas.

3.1.2. Applying AS and Kd filters

Processing includes reduction to the pole (effectively centering anomalies vertically above the feature concerned), and generation of the analytic signal (to decrease the effects of deep anomalies). The results of applying the RTP and AS filters to the magnetic intensity data are given in Figure 2. After applying Reduction to the Pole filter, the magnetic anomalies, which are shown in warm colors in Figure2, are moved a little towards the north to be placed vertically above the related intrusions. Besides, by implementing the analytical signal on the RTP map, the effects of profound anomalies are diminished, while the surface anomalies shown in warm colors probably indicate the hydrothermal regions in bold so that the probable resources of anomalies are correctly located.

In this research work, the Kd ratio, as previously mentioned, was applied to identify the alteration regions related to the hydrothermal activities. Then the regions with various alterations possibility were extracted and presented on a map, as shown in Figure 3. The resulting map, which is an expression of potassium distribution, shows higher quantities of K in warm colors in contrast to the cold colors indicating a low quantity of K distribution, which can be related to the hydrothermal activities. Hence, in order to confirm the probable alteration zones, a further investigation by the Hyperion analysis is required.
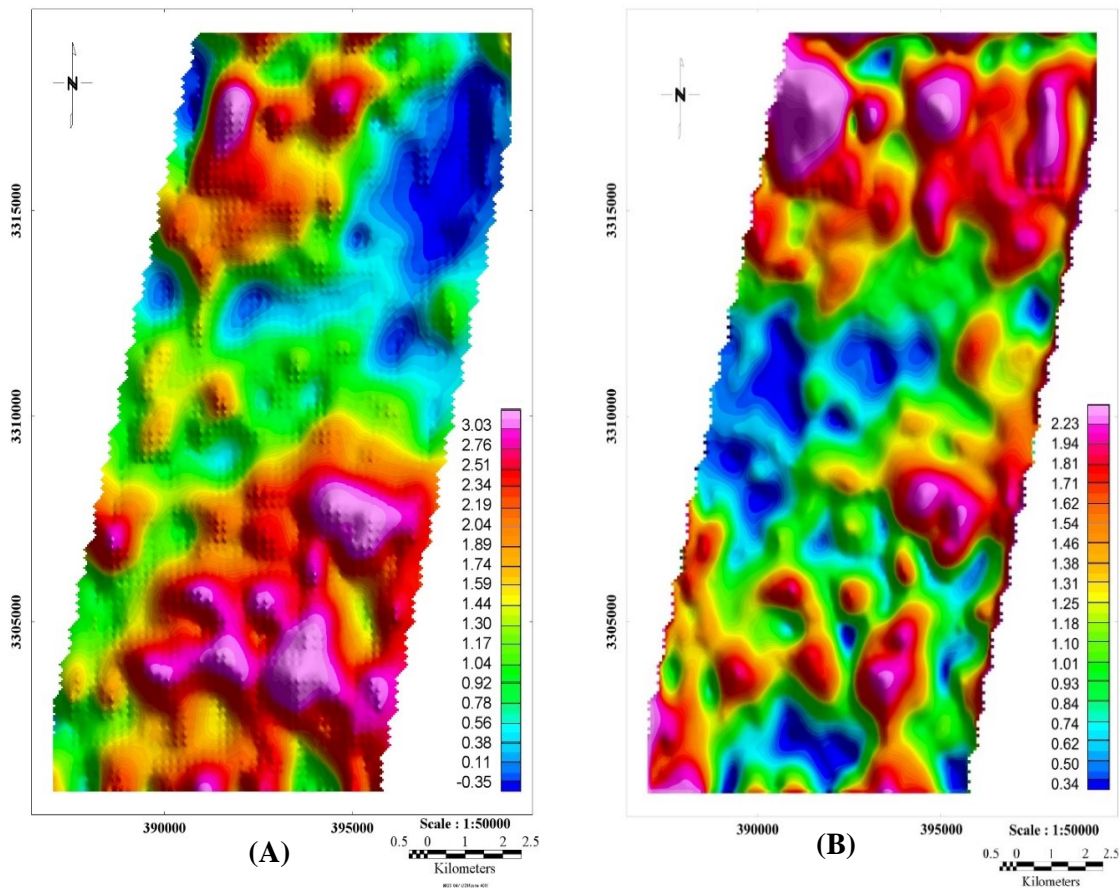

Figure 2. A) Reduced-to-pole map (in terms of gamma) B) Analytic signal map extracted from total magnetic intensity map.

3.2. Analysis on EO-1 hyperion data
3.2.1. Pre-processing

Among the sensors embedded in Earth Observing-1 (EO-1) spacecraft, the specific sensor named Hyperion provides a high resolution hyperspectral imager capable of resolving 242 spectral bands (from 0.4 to 2.5 µm) with a 30-m resolution. The instrument that has two spectrometers in the visible near-infrared (VNIR) and short-wave infrared (SWIR) can image a 7.5 km by 100 km land area per image. The Hyperion L1R dataset, downloaded from USGS and used in this work, was recorded over the studied area in the summer of 2004.

The first unavoidable step was pre-processing. However, the Hyperion dataset had 242 spectral bands but only 198 bands were calibrated, and the rest were set to zero. In addition to the existing four spectral bands (56, 57, 77, 78) in the overlapped region between the VNIR and SWIR spectrometers, the spectral bands 77 and 78 according to the high level of noise were removed. Thus after removing the uncalibrated and water vapor attraction bands, since striping existed in a number of the image bands, implementing a de-stripe algorithm was necessary [23, 24]. To this end, first, the bad lines in which all pixels were set to zero were determined by MATLAB coding and replaced by meaning the around lines. Then by using the vertical stripe removal tool in the ENVI software [25], the rest of the bad lines were corrected.
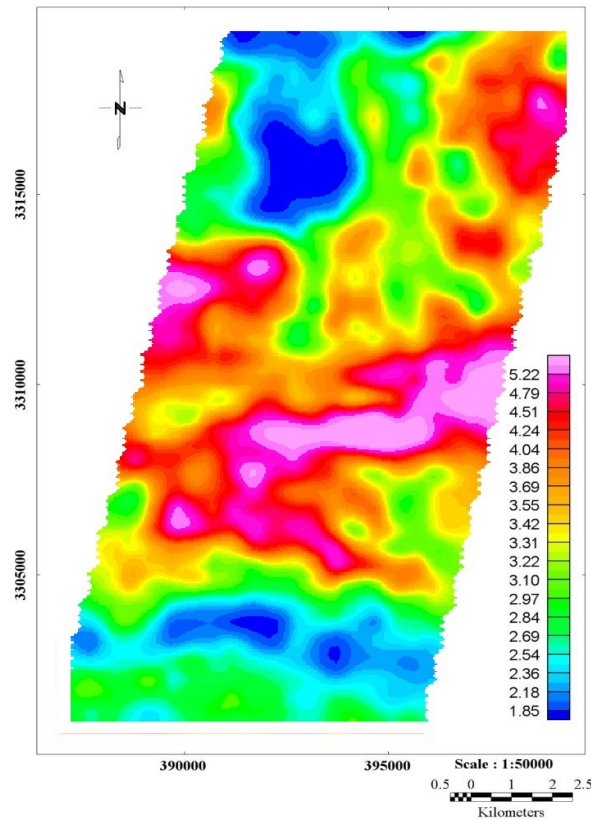

Figure 3. Kd ratio (%) map with various intensities

The other issue affecting the Hyperion data is the spectral curvature effect, also known as the smile or frown curve. This effect is a spectral distortion generated due to the distance between the across track wavelengths and the central wavelength in push-broom sensors. Since the estimation of smile effect regarding its variation from one scene to another is not possible in advance, we should deal with it after obtaining the data and by investigating them. One of the most common methods available to confirm the presence of smile effect in Hyperion data is to exist a brightness gradient in the first eigenvalue image at the MNF space. The MNF algorithm was utilized on the data before and after implementing the cross-track illumination correction tool in the ENVI software to remove the smile effect (Figure 4).

The Hyperion radiance data was converted to surface reflectance using the Fast Line-of-sight Atmospheric Analysis of Spectral Hypercubes (FLAASH) algorithm. FLAASH makes use of the MODTRAN-4 radiative transfer equation [26]. It converts the hyperspectral radiance data to surface reflectance using information for the water vapor column, surface albedo, aerosol, etc. The last step for smoothing the spectra to be more similar to their spectral library was to implement the EFFORT polishing and MNF smoothing.

At last, in order to assess the pre-processing steps, the green vegetation spectra were performed in four levels of pre-processing: without pre-processing, before implementing atmospheric correction, impressed by the FLAASH algorithm, and after smoothing (Figure 5).
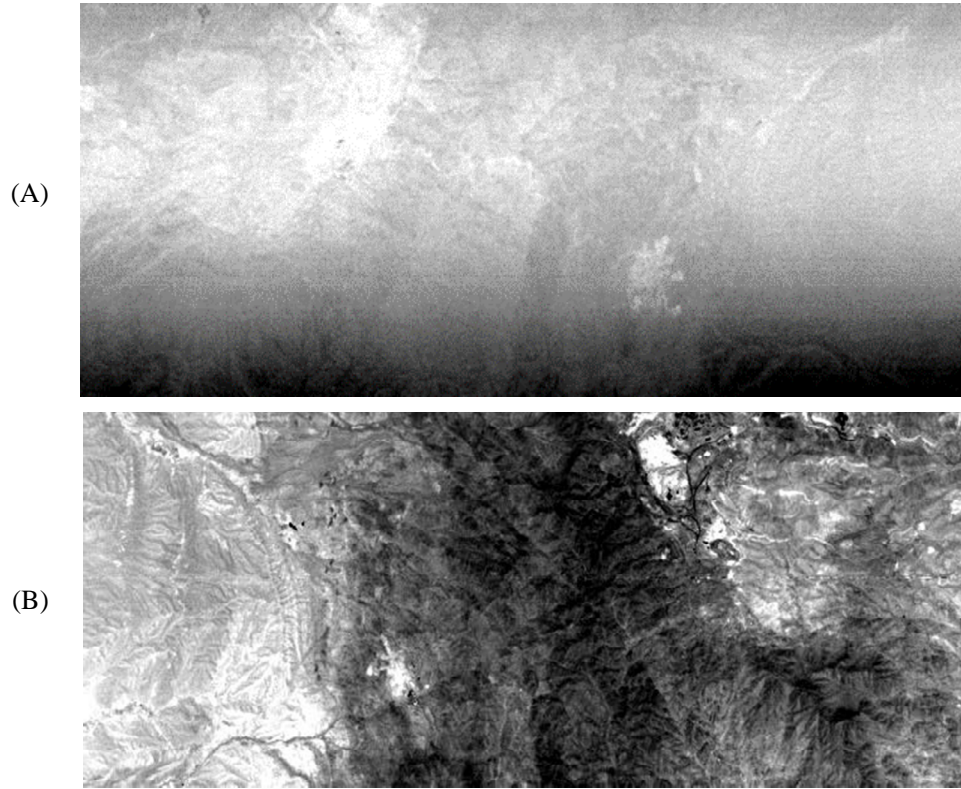
409

(A)

(B)

Figure 4. First eigenvalue image of MNF transformation A) before and B) after removing smile effect

3.2.2. Endmember extraction

During the last decade, many Endmember Extraction Algorithms (EEAs) such as Pixel Purity Index (PPI), Manual Endmember Selection Tool (MEST), N-FINDER, and Iterative Error Analysis (IEA) have been proposed for the aim of autonomous/supervised endmember selection from hyperspectral scenes [27].

One of the most popular EEAs is the PPI algorithm developed by Boardman *et al*. to search for a set of vertices of a convex geometry in a given dataset that is supposed to represent the pure signatures present in the data [28]. PPI has been widely used due to its publicity and availability provided by ENVI developed by the research systems [29].

As mentioned in Table 2, implementing the Minimum Noise Fraction (MNF) algorithm is obligatory. Therefore, first, a "noise-whitening" and dimensionality reduction step was performed using the MNF transform. Then the PPI algorithm was employed on the 20 first MNF images (according to the cut-off point), and n-dimensional visualization was applied to the Region of Interest (ROI) on the MNF images to extract pure pixels and determine their spectra one can see as Figure 6.

The extracted spectra after comparing to the existed USGS spectral library in the ENVI and being labeled were used as the reference spectra for the rest of processing.

Table 2. The features of PPI algorithm [28]

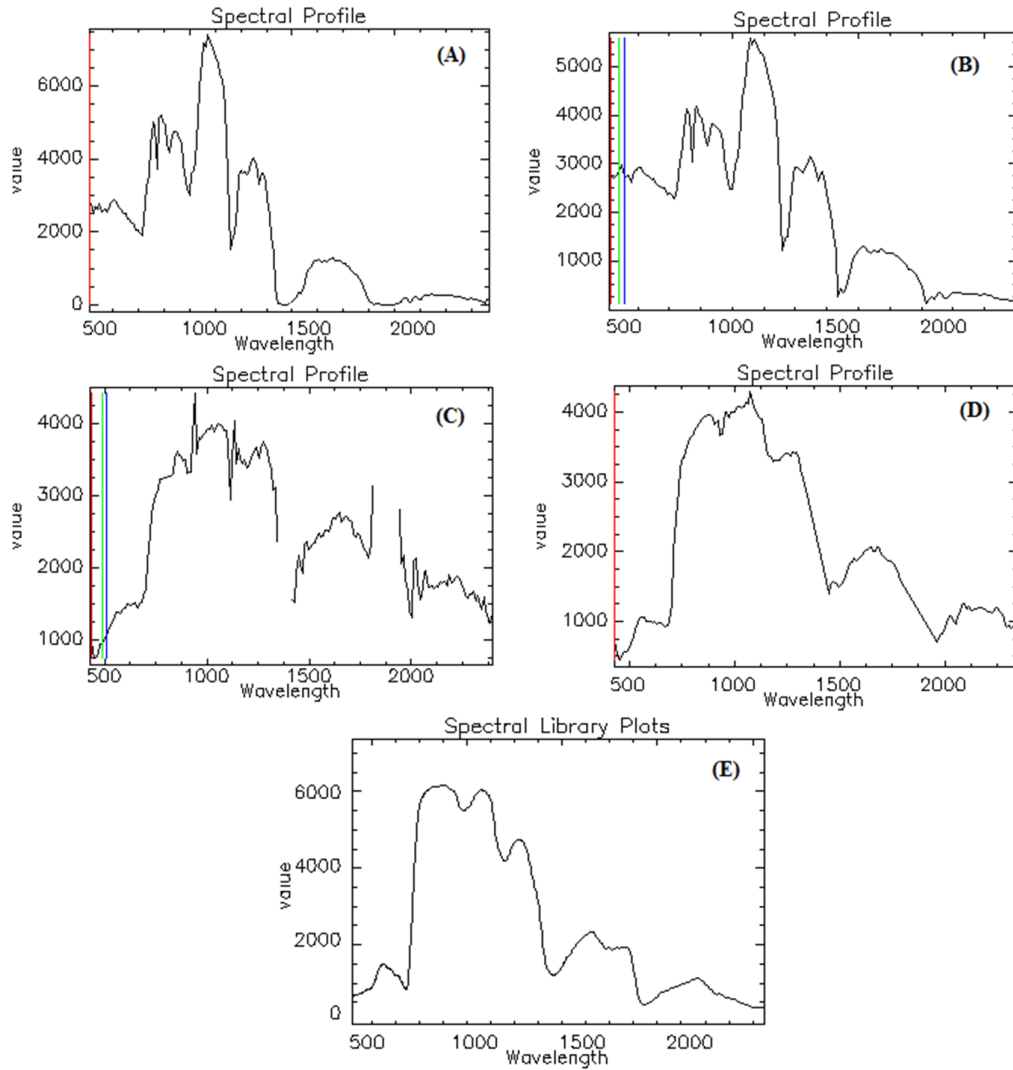| Method	Nature of algorithm	Algorithm assumptions	Computational complexity	Convergence property	Most probable applications
PPI	Supervised, partially interactive	MNF-based reduction in the data	High number of iterations required	Maximum number of iterations	Land-cover and mineral mapping

Figure 5. Spectra of green vegetation extracted from A) Image without any pre-processing B) Image before implementing atmospheric correction C) Image impressed by FLAASH algorithm D) Image after MNF smoothing E) USGS spectral library.
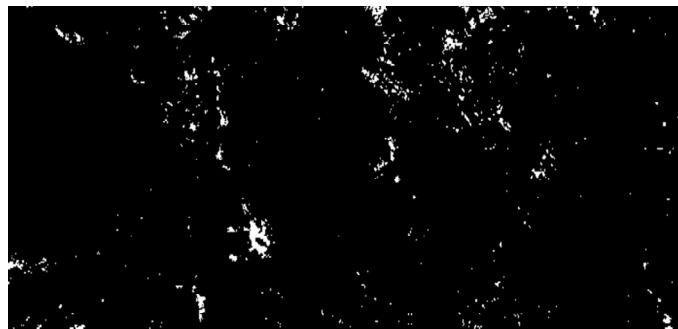

Figure 6. PPI image of the studied area

3.3.3 Applying the SAM algorithm

Spectral Angle Mapper (SAM) is a supervised classification method, which is a tool for a rapid mapping of the spectral similarity of image spectra to the reference spectra. The method compares the angle between the endmember spectrum vector and each pixel vector in n-dimensional space. The result of the comparison is reported as the angular difference (in radians) between the two spectra according to the equation 3:

$$\alpha = \cos^{-1}\left[\frac{\sum_{i=1}^{nb} t_i\, r_i}{\left(\sum_{i=1}^{nb} t_i^{2}\right)^{\frac{1}{2}}\left(\sum_{i=1}^{nb} r_i^{2}\right)^{\frac{1}{2}}}\right] \qquad (3)$$

Here, nb is the number of bands in the image. Each pair of spectra is treated as a vector in nb-space, allowing the similarity of the spectra to be determined without considering their relative brightness values [30].

Hence, the extracted spectra were introduced to the algorithm in order to identify the alteration minerals and generate thematic mineral maps. It is noticeable that geometric correction, because of resampling the original Digital Number (DN) values, was performed after implementing the SAM algorithm.

4. Discussion

Figures 7 to 9 show the alteration maps produced using the Hyperion data; the reference spectra were chosen from the image as an endmember. According to the four extracted spectra indicating argillic, phyllic, propyllitic, and potassic alterations, four alteration maps were generated.

As it can be observed, each pixel may contain more than one mineral. It is remarkable that this trend is reasonable and a mixture of various minerals mainly exists in a unique alteration zone. However, the large size of the pixels of Hyperion data makes mixture pixels unavoidable. The airborne magnetic data was analyzed by applying the analytical signal. In relation to the porphyry copper deposits, very high or very low values in the SA map do not show the altered area, and only the regions with mean values may be associated with the altered minerals; however, it is required to be further investigated.

By comparing the known mines and deposit in the region, Figure 10, with the obtained results by applying the mentioned methods it revealed that, as expected, not all the higher K radiometric values were entirely associated with the hydrothermal alteration zones. While hydrothermal alteration can engender potassic zones pertinent to intrusive stock (granite-granodiorite), some of these zones having a high level of potassium are related to the lithologies that are rich in K-bearing feldspars, and they do not show any alteration area. The results of processing the Hyperion data highlighted the area related to the potassic zone (one of the most important alteration zones) with better precision. Hence, although using such geophysical data will limit the studied area and reduce the time and cost imposed by manual data inspection in the exploration process, their results must be further investigated by field observation, use of remotely-sensed data, and so on.
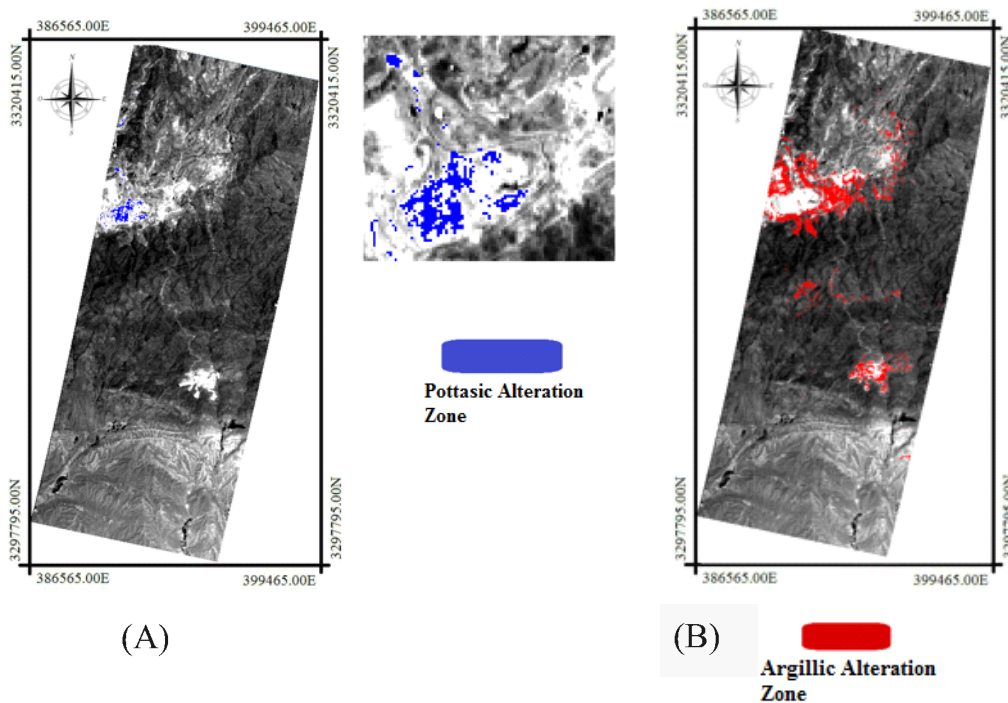

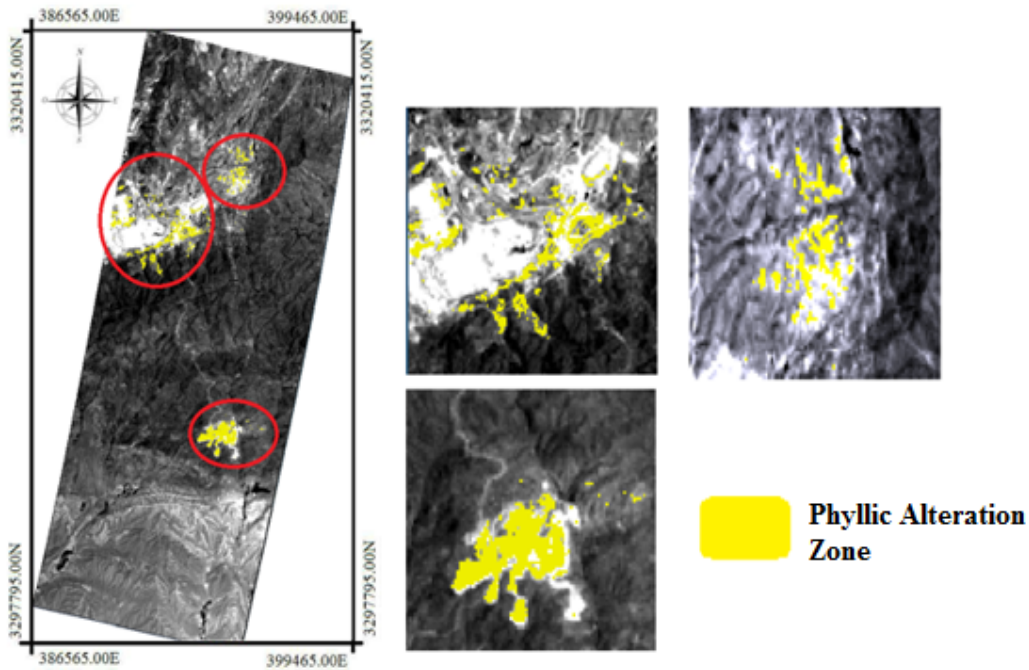**Figure 7. A) Potassic B) Argillic alteration mineral map**
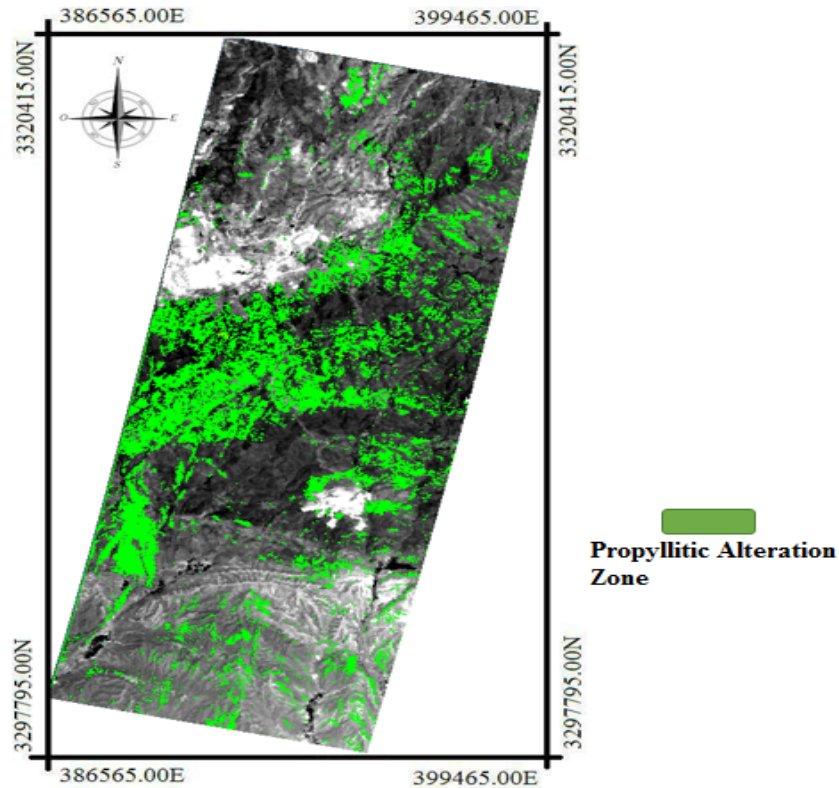
Figure 8. Phyllic alteration mineral map

Figure 9. Propyllitic alteration mineral map

Due to the fact that the region of interest is located in well-exposed terrains, it was quite possible to use the remotely-sensed data. Since the Hyperion imagery contains the SWIR region, which provides abundant mineral information based on analysis of electronic absorption features in mineral groups, analyzing them reveals a great deal of invaluable and helpful information. Therefore, by processing

the Hyperion data, the much striking four alteration maps are produced.

As it was expected and mentioned in the geology overview, the part 2, in the output maps, it is apparently observed that the concentration of alteration zones, at Sarcheshmeh, from the center to outward contain potassic, phyllic, argillic, and propylitic.

Likewise, the discriminated areas successfully corresponded to the alteration zones around Sarcheshmeh, Darrehzar, and Sereidun (Figures. 7–10). Thus it can be concluded that the Hyperion data provides some advantage over the geophysical data such as radiometry or magnetic maps in facilitating a detailed and comprehensive study of the alteration minerals with fairly less requirement of field and laboratory measurements. However, this point should be taken into consideration that gathering field samples definitely leads us towards more accurate results.
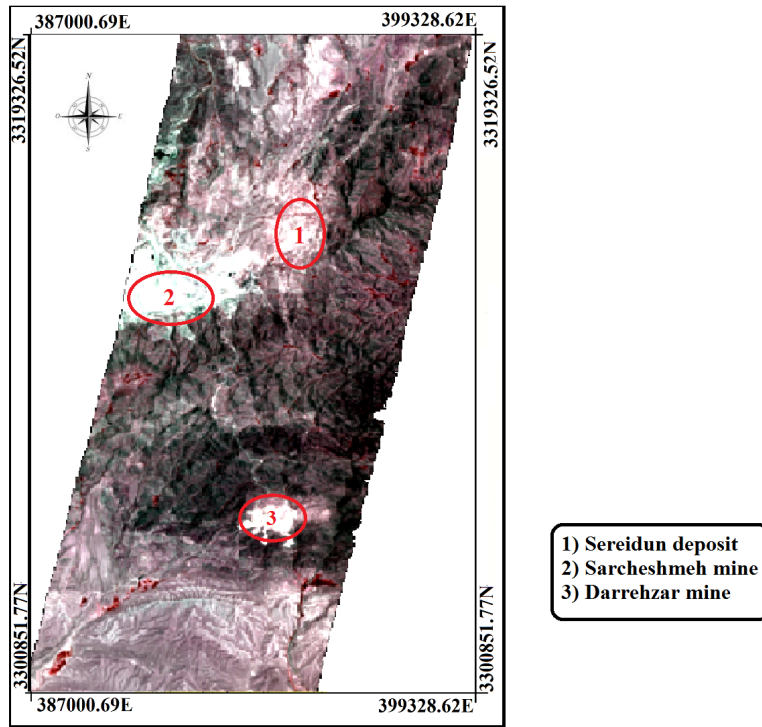

Figure 10. Locations of porphyry copper deposits in the area of interest

5. Conclusions

In this research work, in order to investigate the alteration zone mapping, the magnetic and radiometric data (as geophysical data) and the Hyperion imagery (as remotely-sensed data) were utilized. In relation to the geophysical data, the results of applying two filters, namely analytical signal and Kd ratioing, were analyzed to delineate the probable regions of alteration. It is remarkable that finding an altered area related to the porphyry deposits only by using a geophysical map, and without any ground data, is difficult and may be mistakable.

Thus this requires field investigations, laboratory analysis, and so on to be more reliable. In this work, we applied the Hyperion imagery to lead us to more precise and accurate outcomes. In this way, after applying pre-processing to the Hyperion data and extracting and labeling the endmembers, the Hyperion imagery was classified by four extracted endmembers, and the alteration maps were produced. In order to be more comparable, a detailed union map of the spatial distribution of argillic, phyllic, and potassic alteration maps was obtained in the region of interest. To assess the results and check the veracity, the locations of the former known deposits in this region were compared with the obtained results. As shown in Figure 10, it is evident that the predicted locations of porphyry systems closely match the known mines and deposit.

Similarity, the overall evaluation of the satellite and geophysical data showed that the Hyperion data was more accurate than the geophysical data in this area in terms of hydrothermal alteration mapping. Nevertheless, this point should be taken into consideration that the geophysical data can detect both surface and deep anomalies in contrast

to the Hyperion imagery, which can purely detect the surface features. The combined use of both datasets on condition of having high resolution geophysical and remotely-sensed data as well as some field working is recommended for further studies and hydrothermal alteration mapping.

References

[1]. Moon, C., Whateley, M. and Evans, A. (2000). Introduction to Mineral Exploration. Blackwell, Oxford 498 pp.

[2]. Van der Meer, F.D., Van der Werff, H.M., Van Ruitenbeek, F.J., Hecker, C.A., Bakker, W.H., Noomen, M.F. and Woldai, T. (2012). Multi-and hyperspectral geologic remote sensing: A review. International Journal of Applied Earth Observation and Geoinformation. 14 (1): 112-128.

[3]. Bedini, E. (2011). Mineral mapping in the Kap Simpson complex, central East Greenland, using HyMap and ASTER remote sensing data. Advances in Space Research. 47 (1): 60-73.

[4]. Kruse, F.A., Lefkoff, A.B. and Dietz, J.B. (1993). Expert system-based mineral mapping in northern Death Valley, California/Nevada, using the airborne visible/infrared imaging spectrometer (AVIRIS). Remote Sensing of Environment. 44 (2-3): 309-336.

[5]. Zadeh, M.H., Tangestani, M.H., Roldan, F.V. and Yusta, I. (2014). Sub-pixel mineral mapping of a porphyry copper belt using EO-1 Hyperion data. Advances in Space Research. 53 (3): 440-451.

[6]. Anderson, H. and Nash, C. (1997). Integrated lithostructural mapping of the Rössing area, Namibia using high resolution aeromagnetic, radiometric, Landsat data and aerial photographs. Exploration geophysics. 28 (2): 185-191.

[7]. Graham, D.F. and Bonham-Carter, G.F. (1993). Airborne radiometric data-A tool for reconnaissance geological mapping using a GIS. Photogrammetric Engineering and Remote Sensing. 59 (8): 1243-1249.

[8]. El Nabi, S.H.A. (2013). Role of γ-ray spectrometry in detecting potassic alteration associated with Um Ba'anib granitic gneiss and metasediments, G. Meatiq area, Central Eastern Desert, Egypt. Arabian Journal of Geosciences. 6 (4): 1249-1261.

[9]. Grasty, R.L. and Shives, R.B.K. (1997). Applications of gamma ray spectrometry to mineral exploration and geological mapping. In Workshop presented at Exploration (Vol. 97).

[10]. Lo, B.B. and Pitcher, D.H. (1996). A case history on the use of regional aeromagnetic and radiometric data sets for lode gold exploration in Ghana. In SEG Technical Program Expanded Abstracts 1996 (pp. 592-595). Society of Exploration Geophysicists.

[11]. Wilford, J.R., Bierwirth, P.E. and Craig, M.A. (1997). Application of airborne gamma-ray spectrometry in soil/regolith mapping and applied geomorphology. AGSO Journal of Australian Geology and Geophysics. 17 (2): 201-216.

[12]. Maden, N. and Akaryalı, E. (2015). Gamma ray spectrometry for recognition of hydrothermal alteration zones related to a low sulfidation epithermal gold mineralization (eastern Pontides, NE Türkiye). Journal of Applied Geophysics, 122, 74-85.

[13]. Shives, R.B., Charbonneau, B.W. and Ford, K.L. (2000). The detection of potassic alteration by gamma-ray spectrometry—Recognition of alteration related to mineralizationDetecting Ore Using GRS and K Alteration. Geophysics. 65 (6): 2001-2011.

[14]. Daneshfar, B. (1998). An evaluation of indicators of prospectivity and potential mapping of porphyry deposits in middle and southern British Columbia by a GIS study of regional geochemical and other geoscientific data (Doctoral dissertation, University of Ottawa).

[15]. Abedi, M., Gholami, A. and Norouzi, G.H. (2013). A stable downward continuation of airborne magnetic data: A case study for mineral prospectivity mapping in Central Iran. Computers & Geosciences, 52, 269-280.

[16]. Pazand, K., Hezarkhani, A. and Ataei, M. (2012). Using TOPSIS approaches for predictive porphyry Cu potential mapping: A case study in Ahar-Arasbaran area (NW, Iran). Computers & Geosciences, 49, 62-71.

[17]. Waterman, G.C. and Hamilton, R.L. (1975). The Sar Cheshmeh porphyry copper deposit. Economic Geology. 70 (3): 568-576.

[18]. Lowell, J.D. and Guilbert, J.M. (1970). Lateral and vertical alteration-mineralization zoning in porphyry ore deposits. Economic Geology. 65 (4): 373-408.

[19]. Hoover, D.B., Klein, D.P., Campbell, D.C. and du Bray, E. (1995). Geophysical methods in exploration and mineral environmental investigations. Preliminary compilation of descriptive geoenvironmental mineral deposit models. US Geological Survey Open-File Report, 95-831.

[20]. Nabighian, M.N. (1984). Toward a three-dimensional automatic interpretation of potential field data via generalized Hilbert transforms: Fundamental relations. Geophysics. 49 (6): 780-786.

[21]. Nabighian, M.N. (1972). The analytic signal of two-dimensional magnetic bodies with polygonal cross-section: its properties and use for automated anomaly interpretation. Geophysics. 37 (3): 507-517.

[22]. de Quadros, T.F., Koppe, J.C., Strieder, A.J. and Costa, J.F.C. (2003). Gamma-ray data processing and integration for lode-Au deposits exploration. Natural Resources Research. 12 (1): 57-65.

[23]. Van Ede, R. (2004). Destriping and geometric correction of an ASTER level 1a image. Department of Physical Geography, Utrecht University.

[24]. Darmawan, A. (2006). Mapping soil mineral using Hyperion imagery in relation to the level of structural damage in the Bam earthquake. University of Melbourne, Department of Geomatics.

[25]. Research Systems Inc. (2003). ENVI Tutorial, ENVI Software Package Version 4.0.

[26]. Matthew, M.W., Adler-Golden, S.M., Berk, A., Richtsmeier, S.C., Levine, R.Y., Bernstein, L.S. and Ratkowski, A.J. (2000). Status of atmospheric correction using a MODTRAN4-based algorithm. In Algorithms for multispectral, hyperspectral, and ultraspectral imagery VI (Vol. 4049, pp. 199-207). International Society for Optics and Photonics.

[27]. Plaza, A., Martínez, P., Pérez, R. and Plaza, J. (2004). A quantitative and comparative analysis of endmember extraction algorithms from hyperspectral data. IEEE transactions on geoscience and remote sensing. 42 (3): 650-663.

[28]. Boardman, J.W. (1994, August). Geometric mixture analysis of imaging spectrometry data. In Proceedings of IGARSS'94-1994 IEEE International Geoscience and Remote Sensing Symposium (Vol. 4, pp. 2369-2371). IEEE.

[29]. Chaudhry, F., Wu, C.C., Liu, W., Chang, C.I. and Plaza, A. (2006). Pixel purity index-based algorithms for endmember extraction from hyperspectral imagery. Recent advances in hyperspectral signal and image processing, 37 (2): 29-62.

[30]. Richards, J.A. and Richards, J.A. (1999). Remote sensing digital image analysis (Vol. 3, pp. 10-38). Berlin et al.: Springer.

بررسی نگاشت مناطق آلتراسیون با استفاده از تصاویر سنجنده هایپریون و داده‌های ژئوفیزیک هوایی

مریم لطفی[1]، حسین عارفی [1]* و عباس بحرودی [2]

1- دانشکده مهندسی نقشه برداری و اطلاعات مکانی، پردیس دانشکده های فنی، دانشگاه تهران، تهران، ایران

2- دانشکده مهندسی معدن، پردیس دانشکده های فنی، دانشگاه تهران، تهران، ایران

* نویسنده مسئول مکاتبات:hossein.arefi@ut.ac.ir

چکیده:

از آنجایی که سنجش از دور فراطیفی داده‌های بازتاب شده و تشعشعی را در تعداد زیادی باندهای طیفی باریک و پیوسته ثبت می‌کند، دارای اطلاعات زیادی در زمینه شناسایی و نگاشت مناطق معدنی است. از سوی دیگر، داده‌های ژئوفیزیکی و زمین‌شناسی اطلاعات مفید دیگری درباره‌ی ویژگی‌های فیزیکی خاک و مواد معدنی در اختیار ما می‌گذارند. منطقه‌ی معدنی سرچشمه که در بخش شمال غربی کمربند ماگمایی ارومیه-دختر و درون بخش مرکزی ایران واقع شده‌است، به طور عمده از نوع پورفیری بوده و با مناطق آلتراسیون هیدروترمال همراه اسـت. به دلیل آب و هوای نسـبتا خشـک و همچنین فراوانی رخنمون‌ها، منطقه مورد مطالعه برای کاربردهای سنجش از دوری بسیار مناسب است. در این پژوهش ما بر روی تولید نقشه‌های آلتراسیون در مناطق حاوی نهشته‌های مس پورفیری با بهره‌گیری از اعمال الگوریتم نگاشت کننده زاویه طیفی بر روی تصاویر سنجنده هایپریون و فیلترهای برگردان به قطب و سیگنال تحلیلی بر روی نقشه شدت مغناطیس و تولید نقشه Kd از داده‌های رادیومتری تمرکز نموده‌ایم. لازم به ذکر اسـت که اعمال پیش‌پردازش‌های مناسب بر روی تصاویر سنجنده هایپریون به سبب نسبت پایین سیگنال به نویز بسیار حائز اهمیت است. با مقایسه نهشته‌های معدنی شناخته شده در منطقه مذکور با نتایج به‌دست آمده از این پژوهش مشخص شد که همه‌ی مقادیر بالای پتاسیم در نقشه‌ی رادیومتری بیانگر مناطق آلتراسیون هیدروترمال نیست. اما در مقابل، نقشه‌ی آلتراسیون پتاسیک حاصل شده از بررسی تصاویر هایپریون بطور بسیار مناسبی منطبق بر مناطق آلتراسیون اطراف منطقه معدنی مس سرچشمه بود. در نهایت، صحت نتایج بدست آمده به کمک پردازش تصاویر سنجنده هایپریون با اندیس‌های مس موجود در منطقه تایید شد.

کلمات کلیدی: تصاویر فراطیفی، داده‌های ژئوفیزیکی، مناطق آلتراسیون، الگوریتم نگاشت کننده زاویه طیفی، تصاویر هایپریون.